scientific reports

Check for updates

OPEN

TUBB4B is essential for the expansion of differentiating spermatogonia

Urikhan Sanzhaeva[1], Natalie R. Wonsettler[1], Scott B. Rhodes[1] & Visvanathan Ramamurthy[1,2]✉

Microtubules, polymers of αβ-tubulin heterodimers, are essential for various cellular processes. The incorporation of different tubulin isotypes, each encoded by distinct genes, is proposed to contribute to the functional diversity observed in microtubules. However, the functional roles of each tubulin isotype are not completely understood. In this study, we investigated the role of the β4B-tubulin isotype (*Tubb4b*) in spermatogenesis, utilizing a *Tubb4b* knockout mouse model. We showed that β4B-tubulin is expressed in the germ cells throughout spermatogenesis. β4B-tubulin was localized to cytoplasmic microtubules, mitotic spindles, manchette, and axonemes of sperm flagella. We found that the absence of β4B-tubulin resulted in male infertility and failure to produce sperm cells. Our findings demonstrate that a lack of β4B-tubulin leads to defects in the initial stages of spermatogenesis. Specifically, β4B-tubulin is needed for the expansion of differentiating spermatogonia, which is essential for the subsequent progression of spermatogenesis.

Microtubules composed of αβ-tubulin heterodimers are essential for various cellular processes. One of the primary functions of microtubules is forming mitotic/meiotic spindles, the structures critical for chromosome segregation during cell division[1]. Additionally, microtubules serve as tracks for motor proteins, carrying organelles and vesicles essential for intracellular transport[2]. Furthermore, microtubules form axoneme of cilia and flagella, organelles responsible for sensing the extracellular environment and facilitating motility. The diverse functions of microtubules are regulated through microtubule interactions with microtubule-associated proteins, incorporation of different tubulin isotypes encoded by various genes into microtubules, and posttranslational modifications of tubulins. Despite the fundamental roles of tubulin, mutations in tubulin genes in humans can lead to tissue-specific defects, such as brain malformations, infertility, or impairments in hearing and vision[3–6]. Moreover, studies in various species and the association of distinct tubulin isotypes with specific human diseases indicate specialized roles for tubulin isotypes[7,8].

Spermatogenesis is a process in which germ cells proliferate and differentiate to form sperm within the seminiferous tubules of testes. This process encompasses different stages: mitotic divisions of spermatogonia, meiotic division of spermatocytes, and spermiogenesis (Fig. 1A). Both undifferentiated and differentiating spermatogonia undergo mitotic divisions. Undifferentiated spermatogonia, which includes spermatogonial stem cells, divide to maintain the stem cell pool and produce cells committed to differentiate to support continuous sperm production. These undifferentiated spermatogonia undergo a series of mitotic divisions to yield differentiating spermatogonia. The proliferation of spermatogonia is followed by the meiotic division of spermatocytes that produces round spermatids. Next, these round spermatids differentiate during spermiogenesis and transform into sperm cells[9,10]. Throughout these stages of spermatogenesis, various microtubule structures play roles, including mitotic and meiotic spindles during cell divisions and the manchette and axoneme of sperm flagella during spermiogenesis[11,12].

Interestingly, a study using an antibody specific to β3-, β4A-, and β4B-tubulins demonstrated β3/4 localization in male germ cells[13]. Furthermore, β4B-tubulin (*TUBB4B*) is the predominant tubulin isotype in human testes, as shown in the Genotype-Tissue Expression portal (https://www.gtexportal.org/home/) (Figure S1). Altogether, these studies suggest a potential role for β4B-tubulin in spermatogenesis. However, the role of β4B-tubulin in spermatogenesis remains unclear and is the focus of this work.

In this study, we investigated the functional role of β4B-tubulin (TUBB4B) in spermatogenesis using *Tubb4b* knockout mice (KO; *Tubb4b*$^{-/-}$). We show β4B-tubulin is expressed in germ cells across spermatogenesis and

[1]Department of Biochemistry and Molecular Medicine, West Virginia University School of Medicine, Morgantown, WV 26506, USA. [2]Department of Ophthalmology and Visual Sciences, West Virginia University School of Medicine, Morgantown, WV 26506, USA. ✉email: ramamurthyv@hsc.wvu.edu

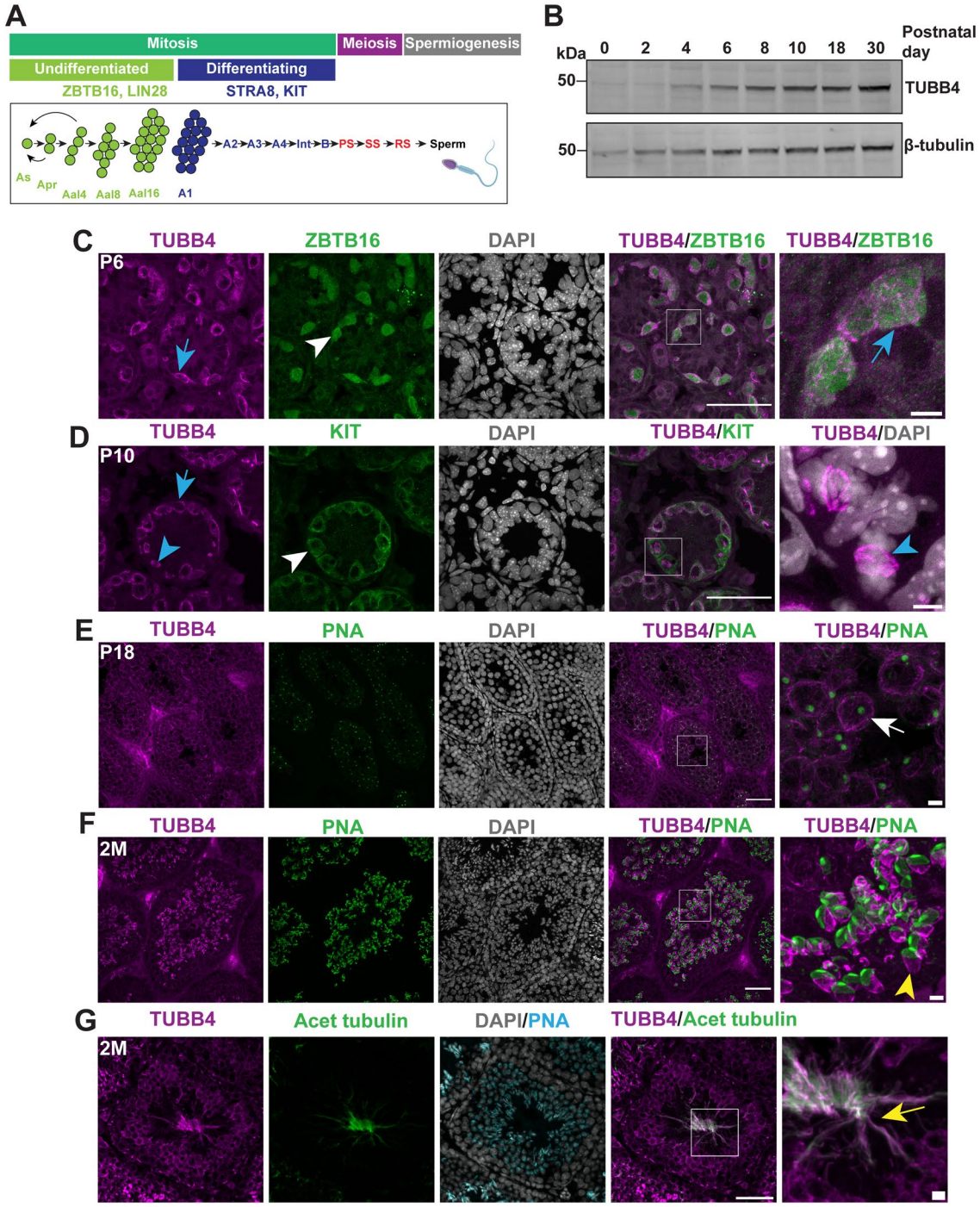

Fig. 1. β4B-tubulin expression during spermatogenesis. (**A**) Schematic of murine spermatogenesis[10]. Key stages and cell types are indicated. Spermatogonia: A_s–A_{single}, A_p–A_{paired}, A_{al}–$A_{aligned}$, *Int* intermediate, *PS* primary spermatocyte, *SS* secondary spermatocyte, *RS* round spermatid. ZBTB16, LIN28-markers of undifferentiated spermatogonia; STRA8, KIT-markers of differentiating spermatogonia. Part of the figure was created with BioRender.com. (**B**) Immunoblot showing β4-tubulin (top) and β-tubulin (bottom) expression in wildtype testes across various stages of spermatogenesis.(**C**–**G**) Cross-sections of wildtype testes at different developmental stages, probed with β4-tubulin antibody (magenta) and various markers of germ cells in green (ZBTB16–undifferentiated spermatogonia marker; KIT–differentiating spermatogonia marker; PNA–acrosomal marker; acet tubulin–sperm flagella marker) and DAPI (gray). White arrowheads point to spermatogonium, white arrows point to round spermatid, cyan arrowheads point to mitotic spindle, cyan arrows point to cytoplasmic microtubules, yellow arrowheads point to the manchette of elongating spermatid, and yellow arrows point to sperm flagellum. *2 M* 2 month-old. Scale bar = 50 μm. Inset scale bar = 5 μm.

is localized to various microtubule-based structures, including cytoplasmic microtubules, spindles, manchette, and axonemes of sperm flagella. We found that male *Tubb4b* knockout mice were sterile and failed to produce sperm. Moreover, the seminiferous tubules in these mice were degenerated, indicating an essential role for β4B-tubulin in male fertility. The absence of β4B-tubulin resulted in a reduction in the number of differentiating spermatogonia. In contrast, the count of undifferentiated spermatogonia remained unchanged. These findings illustrate a critical role for β4B-tubulin in promoting the expansion of differentiating spermatogonia and further progression through spermatogenesis.

Results

Dynamic expression and localization of β4B-tubulin in germ cells throughout spermatogenesis

To investigate the expression of β4B-tubulin during spermatogenesis, we performed immunoblot analysis of lysates from testes of wildtype mice using a β4-tubulin antibody. We observed an increase in β4B-tubulin expression from postnatal day 0 (P0) to P30 as spermatogenesis progressed (Fig. 1B). Immunofluorescence staining of wildtype testes cross-sections with the β4-tubulin antibody at different time points showed expression of β4-tubulin in germ cells, including both undifferentiated (P6) and differentiating spermatogonia (P10). We used ZBTB16 (zinc finger and BTB domain containing 16) and KIT (KIT proto-oncogene receptor tyrosine kinase) as markers for undifferentiated and differentiating spermatogonia, respectively (Fig. 1C,D, marked by a white arrowhead)[14,15]. β4B-tubulin localized to cytoplasmic microtubules and mitotic spindle in spermatogonia (Fig. 1C,D, marked by a cyan arrow and cyan arrowhead). We used peanut agglutinin (PNA) as an acrosomal marker of spermatids[16]. In cross-sections from P18 testes, as spermatogenesis progressed, β4B-tubulin localized to cytoplasmic microtubules of round spermatids (Fig. 1E, marked by a white arrow). As round spermatids were undergoing spermiogenesis, β4B-tubulin was found in the elongating spermatid manchette, a transient skirt-like microtubule-based structure crucial for sperm head shaping (Fig. 1F, marked by yellow arrowhead)[11,12]. α-tubulin was used as a manchette marker to confirm TUBB4B localization (Figure S2). β4B-tubulin was also localized to sperm flagella (Fig. 1G, marked by a yellow arrow). We used acetylated tubulin (acet tubulin) as a marker for flagella (Fig. 1G). These findings collectively demonstrate that β4B-tubulin is expressed in the germ cells throughout spermatogenesis.

β4B-tubulin is essential for male fertility

We discovered that *Tubb4b*$^{-/-}$ homozygous males were infertile as they failed to produce litters during the generation of *Tubb4b*$^{-/-}$ mice, indicating the essential role of β4B-tubulin in male fertility. Immunoblot analysis using lysates from testes at P30 *Tubb4b*$^{-/-}$ and littermate controls probed with β4-tubulin antibody confirmed the absence of β4B-tubulin in the *Tubb4b*$^{-/-}$ testes (Fig. 2A), indicating that β4B-tubulin is the predominant β4-tubulin isotype expressed in testes. Additionally, we noted a roughly 60% reduction in the overall β-tubulin level in mutant testes (p-value = 0.02) (Fig. 2A). Hematoxylin and eosin (H&E) staining of testes and cauda epididymis from 2-month-old wildtype and *Tubb4b*$^{-/-}$ littermates revealed degenerated seminiferous tubules and a complete absence of sperm cells in testes and cauda epididymis (where matured sperms are stored) in the absence of β4B-tubulin, suggesting defects at an early stage of spermatogenesis (Fig. 2B). Moreover, *Tubb4b*$^{-/-}$ testes were drastically smaller than littermate controls (Fig. 2C). To pinpoint the onset of these spermatogenesis defects, we analyzed the testes of *Tubb4b*$^{-/-}$ and control mice using H&E staining at earlier developmental stages. At P6, the testes cross-section from control and *Tubb4b*$^{-/-}$ mice were similar (Fig. 2D, top panel). At P15, meiotic cells were absent, and cells with condensed nuclei, indicative of apoptosis, were present in the seminiferous tubules of mutant mice (Fig. 2D, bottom panel, arrowheads), pointing to early defects in spermatogenesis, potentially during the early mitotic expansions of germ cells. Furthermore, a significant difference in testes weight was observed at P10 (p-value = 0.01) but not at P6 (Fig. 2E). Altogether, these findings point to an essential role of β4B-tubulin in male fertility, and its absence leads to defects in spermatogenesis and subsequent failure to produce sperm.

β4B-tubulin deficiency leads to reduced differentiating spermatogonia.

To determine when defects in spermatogenesis begin in testes lacking β4B-tubulin, we analyzed transcript levels of markers for undifferentiated and differentiating spermatogonia in P10 testes (Fig. 3A). mRNA levels of undifferentiated spermatogonia markers, *Zbtb16* and *Lin28*, Refs.[14,15,17] were similar to control (Fig. 3A). In contrast, the mRNA levels of differentiating spermatogonia markers, *Kit* and *Stra8*, Refs.[15,18] were significantly reduced in testes lacking β4B-tubulin (p-value = 0.01 and 0.02 respectively), indicating that β4B-tubulin is essential for the expansion of differentiating, but not undifferentiated, spermatogonia. To confirm these findings, we immunostained P10 testes cross-sections with a marker of undifferentiated or differentiating spermatogonia (ZBTB16 or KIT, respectively) and quantified the number of undifferentiated and differentiating spermatogonia per seminiferous tubules in the mutant and control testes (Fig. 3B,C). Indeed, analysis of P10 testes cross-sections immunostained with KIT, a marker of differentiating spermatogonia, revealed a significant decrease in the number of differentiating spermatogonia (KIT^{+} cells) per seminiferous tubule (p-value = $1.9^{*}10^{-65}$) (Fig. 3D, right panel). In contrast, the number of undifferentiated spermatogonia per seminiferous tubule (ZBTB16^{+} cells) was similar to wildtype littermates (Fig. 3D, left panel). Altogether, these findings show a requirement for β4B-tubulin isotype for the expansion of differentiating spermatogonia and for the progression of spermatogenesis.

TUBB4B R391C mutation acts in a dominant negative manner

We also developed the *Tubb4b* R391C knock-in mouse model, carrying the same mutation found in patients with vision and hearing loss. Interestingly, the heterozygous *Tubb4b* knock-in (R391C/+) mouse model exhibited male infertility. Consequently, we were unable to expand this mouse colony beyond the F1 generation (R391C/+). The

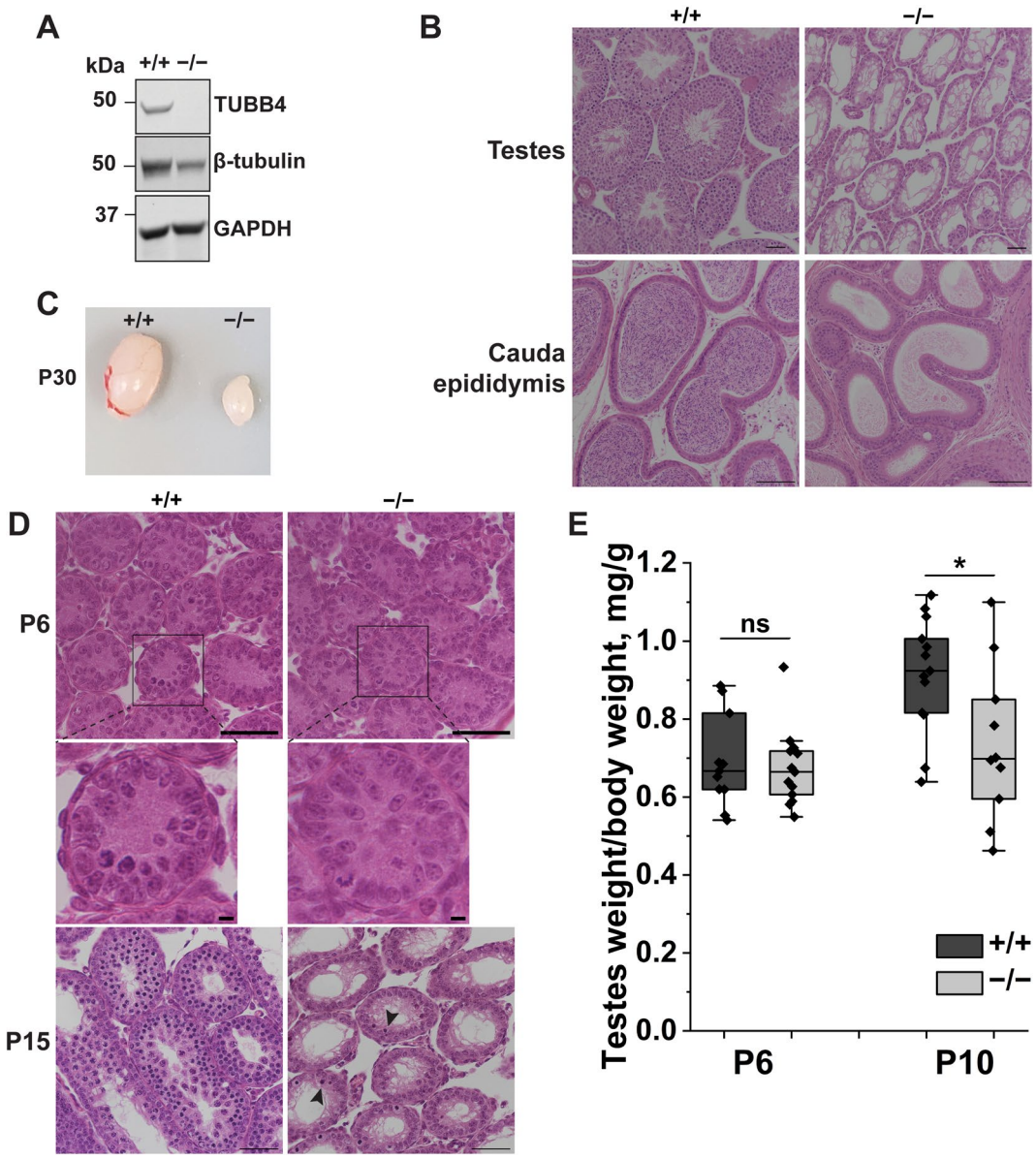

Fig. 2. Loss of β4B-tubulin causes male infertility and degeneration of seminiferous tubule. (**A**) Immunoblot of testes lysates from P30 animals probed with antibodies against β4-tubulin, β-tubulin, and GAPDH (glyceraldehyde 3-phosphate dehydrogenase). GAPDH was used as a loading control. (**B**) Top: Cross-sections of testes from *Tubb4b*$^{+/+}$ and *Tubb4b*$^{-/-}$ littermates at 2 months, stained with hematoxylin and eosin (H&E). Scale bar = 50 µm. Bottom: Cross-sections of cauda epididymis from *Tubb4b*$^{+/+}$ and *Tubb4b*$^{-/-}$ littermates at 2 months, stained with H&E. Scale bar = 50 µm. (**C**) Image of P30 testes from *Tubb4b*$^{-/-}$ and control littermate. (**D**) Top: Cross-sections of testes from *Tubb4b*$^{+/+}$ and *Tubb4b*$^{-/-}$ littermates at P6, stained with H&E. Scale bar = 50 µm. Middle: Higher-magnification images of cross-sections of testes from *Tubb4b*$^{+/+}$ and *Tubb4b*$^{-/-}$ littermates at P6, stained with H&E. Scale bar = 5 µm. Bottom: Cross-sections of testes from *Tubb4b*$^{+/+}$ and *Tubb4b*$^{-/-}$ littermates at P15, stained with H&E. Scale bar = 50 µm. Black arrowheads point to condensed nuclei. (**E**) *Tubb4b*$^{-/-}$ and control testes weight normalized to body weight at P6 and P10. An asterisk (*) denotes significance at $p < 0.05$. All experiments were conducted at least three times with littermates serving as controls (+/+).

testis from the R391C heterozygous mouse was smaller than that from the age-matched C57Bl6J mouse (Fig. 4A). Histological analysis of the testis from heterozygous TUBB4B R391C (TUBB4B R391C/+) mouse revealed the absence of sperm cells in seminiferous tubules (Fig. 4B). Interestingly, unlike the *Tubb4b*$^{-/-}$ mice, spermatocytes were present in R391C/+ testes, suggesting defects at later stages and a dominant negative effect of TUBB4B point mutation on spermatogenesis. Furthermore, H&E staining of testes cross-sections from TUBB4B R391C/+ mouse revealed the absence of spermatocytes beyond the pachytene stage in TUBB4B R391C/+ testis cross-sections (Fig. 4B), suggesting defects in the meiotic progression in this mutant. Besides the defects in spermatogenesis, we also noted Leydig cell hyperplasia in this animal (Fig. 4B). These findings suggest that male patients with

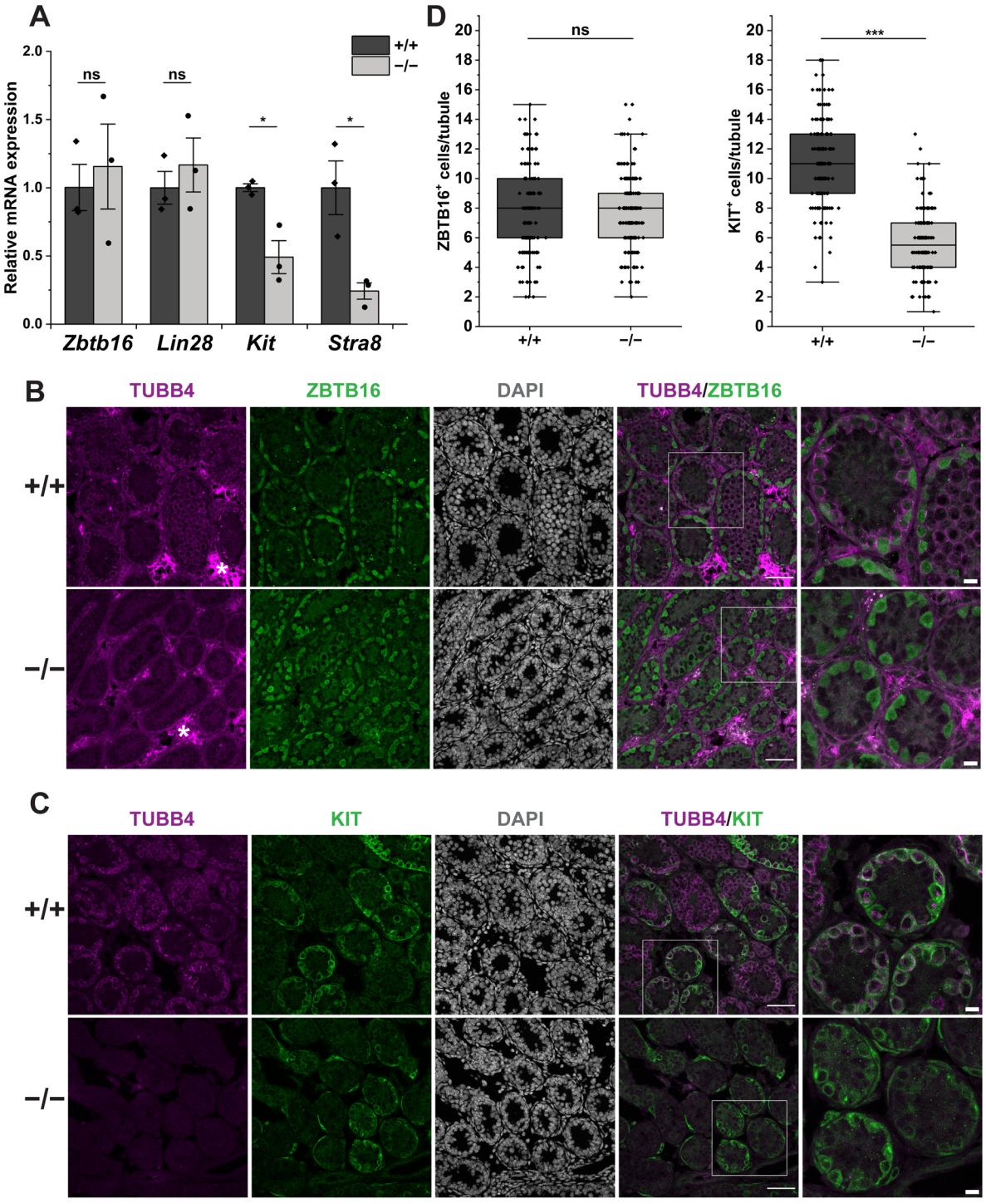

Fig. 3. β4B-tubulin is needed for the expansion of differentiating spermatogonia. (**A**) mRNA levels of markers for undifferentiated spermatogonia (*Zbtbt16*, *Lin28*) and differentiating spermatogonia (*Kit*, *Stra8*) in *Tubb4b*$^{-/-}$ and *Tubb4b*$^{+/+}$ testes at P10. Data are presented as mean ± SEM (n = 3, unpaired two-tailed t-test). An asterisk (*) indicates statistical significance ($p < 0.05$); "ns" denotes not significant. (**B**) Cross-sections of P10 testes from *Tubb4b*$^{-/-}$ and *Tubb4b*$^{+/+}$ mice stained for β4-tubulin (magenta) and ZBTB16 (green, marker for undifferentiated spermatogonia marker). Areas of non-specific staining are marked with an asterisk. Scale bar = 50 µm. Inset scale bar = 10 µm. (**C**) Cross-sections of P10 testes from *Tubb4b*$^{-/-}$ and *Tubb4b*$^{+/+}$ mice stained for β4-tubulin (magenta) and KIT (green, maker for differentiating spermatogonia marker). Scale bar = 50 µm. Inset scale bar = 10 µm. (**D**) Quantification of undifferentiated spermatogonia (ZBTB16^{+} cells) (Left) and differentiating spermatogonia (Right) per seminiferous tubule in P10 testes from *Tubb4b*$^{-/-}$ and control mice. Data analysis was performed using an unpaired two-tailed t-test for three replicates. ***denotes significance of $p < 0.001$; "ns" indicates not significant difference.

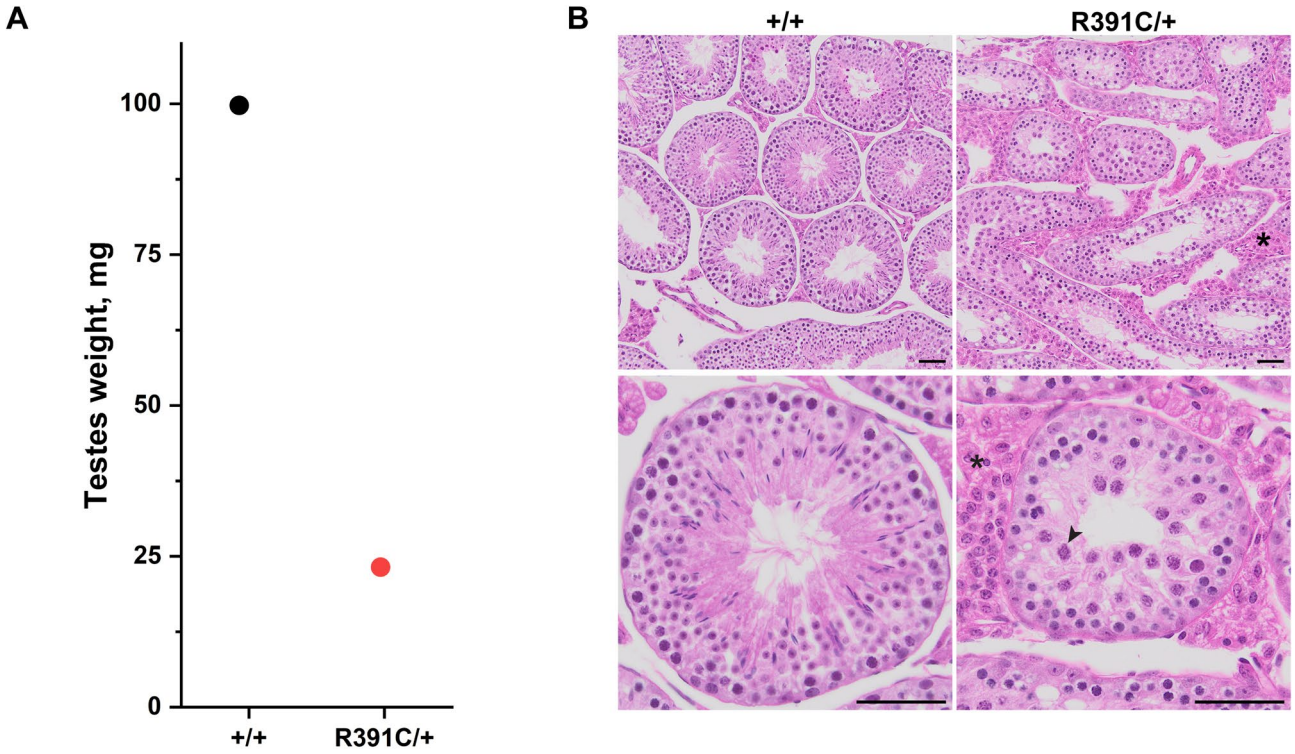

Fig. 4. Tubb4b R319C heterozygous male mouse is sterile. (**A**) Weight of testes from 9.5-month-old Tubb4b R391C heterozygous male and age-matched C57Bl6J. (n = 1, this result is preliminary). (B) Testes cross-section from 9.5-month-old Tubb4b R391C heterozygous male and age-matched C57Bl6J mouse stained with H&E. Black arrowhead points to pachytene spermatocyte. Leydig cell hyperplasia is denoted with an asterisk. Scale bar = 50 µm. (n = 1, this result is preliminary).

TUBB4B mutations should be screened for infertility as *TUBB4B* isotype is the predominant β-tubulin isotype in human testes (Figure S1).

Discussion

Multiples α- and β- tubulin isotypes are encoded in the mammalian genome; however, the functional roles of tubulin isotypes are not fully understood. In this study, we investigated the functional role of β4B-tubulin in spermatogenesis and found that β4B-tubulin is essential for male fertility. We showed that β4B-tubulin is expressed in germ cells throughout spermatogenesis and that its absence leads to loss of sperm production, degeneration of seminiferous tubules, and depletion of differentiating spermatogonia (Fig. 5).

Microtubule-based structures are essential for spermatogenesis as they are involved in germ cell division, sperm head shaping, and the development of flagella[11,12,19]. Indeed, previous studies have demonstrated essential roles for tubulin isotypes and tubulin posttranslational modifications, such as tubulin glutamylation, in spermatogenesis. Studies in *D. melanogaster* have demonstrated an essential role for testis-specific β2-tubulin in spermatogenesis, and mutations in this β-tubulin isotype caused various defects in spermatogenesis, such as failure to progress through meiosis or loss of central pair of sperm flagella[20–22]. Interestingly, α8-tubulin has been implicated to have a role in spermatogenesis[24]. Furthermore, non-canonical ε-tubulin has been shown to be essential in microtubule structures during meiosis and shaping of sperm head[23]. Mice lacking enzymes responsible for tubulin glutamylation or deglutamylation displayed male infertility caused by defects in the development of sperm flagella[25,26].

Previous studies have shown the expression of β3/4-tubulin in the germ cells[13]; however, the significance of β4B-tubulin in spermatogenesis is unknown. The β4-tubulin antibody we used cannot distinguish between β4A- and β4B-tubulin[27]; therefore, we probed protein extracts from the testes of control and *Tubb4b*$^{-/-}$ mice with β4-tubulin antibody. The β4-tubulin was completely absent in *Tubb4b*$^{-/-}$ testes, as demonstrated by immunoblotting, indicating that β4B-tubulin is the predominant β4-tubulin isotype in testes (Fig. 2A). Furthermore, immunostaining of testes cross-sections from *Tubb4b*$^{-/-}$ with β4-tubulin antibody confirmed the absence of β4-tubulin staining in these sections, indicating β4-tubulin signal in these sections corresponds to β4B-tubulin (Fig. 3B,C). Our studies, using β4-tubulin antibody, revealed that β4B-tubulin is expressed in germ cells at various stages of spermatogenesis, including in undifferentiated and differentiating spermatogonia.

In spermatogonia, β4B-tubulin localized to cytoplasmic microtubules and mitotic spindles of differentiating spermatogonia. Although the number of undifferentiated spermatogonia per seminiferous tubules in testes lacking β4B-tubulin was comparable to control littermates, the number of differentiating spermatogonia per seminiferous tubules was significantly reduced. These results show the vital role of β4B-tubulin in the expansion

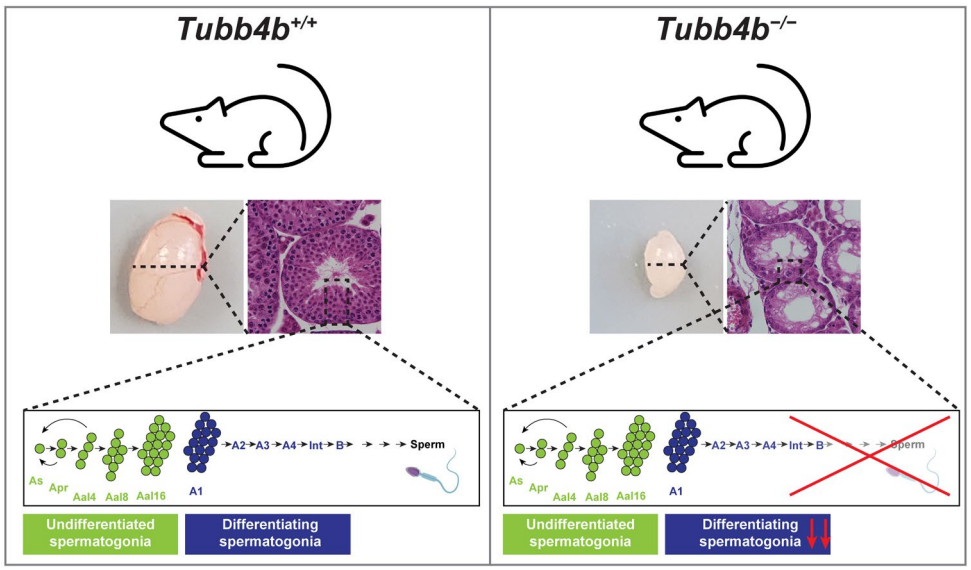

Fig. 5. β4B-tubulin is essential for spermatogenesis. *Tubb4b*$^{-/-}$ male mice are sterile and fail to produce sperm cells. The absence of TUBB4B leads to a reduction in differentiating spermatogonia numbers and failure to progress through spermatogenesis. Part of the figure was created with BioRender.com.

of differentiating spermatogonia. Indeed, the deletion of TUBB4B in spermatogonia cell culture has been shown to slow cell proliferation[28]. The observed defects at the early stages of spermatogenesis in the absence of β4B-tubulin are likely due to its predominant expression in differentiating spermatogonia. Unlike differentiating spermatogonia, in undifferentiated spermatogonia, other β-tubulin isotypes may compensate for the loss of β4B-tubulin. Indeed, scRNA-seq analysis of murine testes identified *Tubb4b* as one of the markers of differentiating spermatogonia, specifically A1-A4 spermatogonia, while *Tubb5* marked the undifferentiated spermatogonia[29]. We speculate that β4B-tubulin does not have a unique function in differentiating spermatogonia, and the defects at this stage of spermatogenesis are solely due to below-optimal tubulin concentration. We hypothesize that the expression of any other tubulin isotype in place of β4B-tubulin could potentially lead to normal expansion of differentiating spermatogonia.

Indeed, in *D. melanogaster*, mutations of the testis-specific β2-tubulin resulted in protein degradation, decreased tubulin concentration, and defective meiosis[20]. Intriguingly, the expression of β1-tubulin instead of testis-specific β2-tubulin resulted in normal meiosis but abnormal sperm axoneme morphology, suggesting distinct functional roles for these tubulin isotypes[21,22]. Our findings and those in *D. melanogaster* suggest that β4B-tubulin may have unique functions in later stages of spermatogenesis, namely in spermiogenesis, as evidenced by its localization to the manchette and axoneme of sperm flagella. Furthermore, recent studies revealed an essential role for β4B-tubulin in axoneme formation in multiciliated cells[30,31]. Unfortunately, the *Tubb4b*$^{-/-}$ mouse model we utilized does not allow us to investigate the specific role of β4B-tubulin in sperm flagellum formation, as the defects occur at the early stage of spermatogenesis prior to spermiogenesis (Fig. 4). Therefore, future research using spermatid-specific conditional *Tubb4b* knockout mouse models will be needed to address the importance of β4B-tubulin in sperm flagellum formation and function.

We also showed that heterozygous TUBB4B R391C/ + male mouse displayed infertility, suggesting the dominant negative effect of TUBB4B point mutation on spermatogenesis. This result is in agreement with a recent study demonstrating male infertility in heterozygous TUBB4B R391H/ + mice due to defects in spermatogenesis[31]. It is worth noting that the *Tubb4b*$^{+/-}$ did not display fertility issues and were used for breeding to generate *Tubb4b*$^{-/-}$ animals. Unlike mice lacking TUBB4B that failed to progress through spermatogenesis due to defects in differentiating spermatogonia, TUBB4B R391C/ + mouse displayed defects in the meiotic progression as spermatocytes beyond the pachytene stage were absent in this animal. Previous studies have shown that β4B-tubulin carrying R391C mutation incorporates into microtubules[4,31] and does not affect cell proliferation[4]. Therefore, it is plausible that TUBB4B R391C/ + differentiating spermatogonia maintain optimal tubulin concentration and are able to differentiate into spermatocytes. However, it is not clear why the R391C mutation in TUBB4B tubulin would lead to failure to progress through meiosis. During the first meiotic prophase, the homologous chromosomes pair and undergo recombination. Interestingly, the chromosomal movement is dependent on the microtubule cytoskeleton[19,32–34]. It has been proposed that microtubule depolymerization and repolymerization contribute to chromosomal movement[33]. Interestingly, recent studies demonstrated that TUBB4B R391C mutation results in a decreased microtubule growth rate and affects microtubule dynamics[4,31]. Thus, TUBB4B R391C mutation may affect chromosome movement in mouse spermatocytes. It is worth noting that we failed to expand the TUBB4B R391C line due to male fertility issues and the results shown in (Fig. 4) are preliminary. Therefore, future studies using a conditional TUBB4B knock-in mouse model would be needed to assess the effect of TUBB4B point mutation on spermatogenesis.

In summary, our studies using the *Tubb4b* murine model found that the β4B-tubulin is essential for male fertility. Specifically, β4B-tubulin is needed for the expansion of differentiating spermatogonia, and its absence leads to impaired spermatogenesis and the depletion of differentiating spermatogonia. Furthermore, we have shown that the heterozygous *Tubb4b* R391C mouse model also displayed fertility due to defects during the meiotic stage of spermatogenesis.

Materials and methods

Ethics statement

All experimental procedures involving animals in this study were conducted in accordance with the Guide for the Care and Use of Laboratory Animals of the National Institutes of Health. All animals were handled and housed following the protocols approved by the institutional animal care and use committee (IACUC) of West Virginia University. All authors complied with the guidelines for animal research: reporting of in vivo experiments (ARRIVE).

Animal model and genotyping

Tubb4b$^{-/-}$ mice in C57BL/6NJ background were obtained from The Jackson Laboratory (Catalog # 43743-JAX). Mutation in *Tubb4b*$^{-/-}$ mice generated by CRISPR-Cas9 resulted in the deletion of exons 2–3 and premature stop codon. We crossed the animals to 129SV/E strain and maintained them in the mixed background. Genotyping for wildtype *Tubb4b* alleles was performed using 5'-TTTGGTGAGTGTGGTGGAGG-3' and 5'-CCTGCCAATGTTCAAGGAGA-3' primers. Genotyping for mutant *Tubb4b* alleles was performed using 5'-TCCCGAAGTGCTCCTCTTCT-3' and 5'-AGACCAGACGGAGATGTACAGA-3' primers. The thermocycling conditions for *Tubb4b* genotyping were 95 °C for 4 min, 35 cycles of 95 °C for 30 s, 55 °C for 30 s, 72 °C for 30 s, and a final extension step of 72 °C for 5 min.

Tubb4b knock-in mice (R391C) were generated using 5'-CACAGCCATGTTCCGACGCA-3' guide RNA (gRNA) and repair oligonucleotides: 5'-TGAAAATGTCGGCCACCTTCATTGGCAACAGCACCGCTATTCAGGAGCTGTTCAAACGCATCTCAGAGCAGTTCACAGCCATGTTCCGATGCAAAGCCTTCCTACACTGGTACACGGGTGAAGGCATGGATGAGATGGAGTTCACTGAGGCTGAGAGCAACATGAACGACCTGGTGTCCGA-3' (R391C). Genotyping for *Tubb4b* point mutations was performed using 5'-AGTGGATCCCCAACAATGTGAA-3' and 5'-ATGCAGGACAACTATGCACTGA-3' primers. The thermocycling conditions were 95 °C for 4 min, 38 cycles of 95 °C for 30 s, 60 °C for 30 s, 72 °C for 30 s, and a final extension step of 72 °C for 5 min. The PCR product sequencing was performed by Psomagen Inc.

Immunoblotting

Mice were euthanized by CO_2 inhalation followed by cervical dislocation. Their testes were then dissected and separated from epididymis and fat. Testes were weighed and immediately frozen in dry ice. The samples were sonicated in phosphate-buffered saline (PBS) containing a protease inhibitor cocktail (Thermo Fisher) and 1 mM dithiothreitol (DTT). Protein concentrations were measured using a NanoDrop spectrophotometer or the BCA protein assay (Thermo Fisher). For analysis, samples were subjected to SDS-PAGE and then transferred onto polyvinylidene difluoride (PVDF) membranes (Immobilon). The membranes were first stained for total protein (LI-COR), then blocked with blocking buffer (LI-COR) for 30 min at room temperature. Overnight incubation of membranes with primary antibodies was performed at 4˚, followed by three 5 min washes in PBST (PBS containing 0.1% Tween-20) at room temperature. Then, the membranes were incubated with secondary antibodies for 30 min at room temperature and washed three times with PBST for 5 min at room temperature. The membranes were imaged using the Odyssey Infrared Imaging System (LI-COR). The density of the protein bands was quantified using ImageJ software. The antibodies used in this study are listed in (Table S1).

Immunofluorescence staining

For immunofluorescence analysis of testicular cross-sections, testes were fixed in 4% paraformaldehyde (PFA) in PBS for 5 h (PN 6–10 testes) or overnight (adult testes). Following fixation, the testes were rinsed three times with PBS and incubated in 20% sucrose in PBS overnight at 4 °C. Testes were then incubated in a 1:1 mixture of 20% sucrose and OCT (Tissue-Tek) for 1 h before being flash frozen in OCT. Testicular sections, 8 µm thick, were cut on Leica CM1860 cryostat, mounted onto superfrost slides, and stored at −20 °C. For staining with tubulin antibodies, epitope retrieval was performed. Epitope retrieval was performed on the sections using 10 mM citrate buffer (pH = 6) for 30–40 min at 95 °C, followed by three 5 min washes with PBS. The sections were then incubated in blocking buffer (10% goat or donkey serum, 0.5% TritonX-100, and 0.05% (w/v) sodium azide in PBS). This was followed by overnight incubation with primary antibodies at the dilutions listed in (Table S1). After washing the sections three times with PBS containing 0.1% TritonX-100 for 5 min each, the sections were incubated with secondary antibodies and DAPI for nuclear staining for 1 h at room temperature. The slides were washed three more times with PBS for 5 min each and mounted using ProLong Gold Antifade reagent (Invitrogen) and coverslipped.

Imaging was performed with a Nikon C2 laser scanning confocal microscope with Plan Apo λ 20x/0.75 NA, Plan fluor 40x/1.30 NA oil, Plan Apo λ 60X/1.40 NA oil, or Plan Apo λ 100x/1.45 NA oil objectives or Nikon Crest V3 spinning disk confocal microscope with Plan Apo λD 20x/0.8 NA objective. All fluorescent images represent maximum intensity projections of z-stack generated using Nikon NIS-Elements software. The antibodies used are listed in (Table S1).

Cell counting
Images of testicular cross-sections from *Tubb4b*$^{-/-}$ and control littermates (n = 3), stained for undifferentiated or differentiating spermatogonia markers, were captured using a Nikon C2 laser scanning confocal microscope with Plan Apo λ 20x/0.75 NA objective or Olympus VS120 Slide Scanner with U Plan S Apo 20x/0.75 NA objective. For the analysis, only round seminiferous tubule cross-sections were selected. Using the ImageJ Cell Counter plugin, we counted cells in at least 50 seminiferous tubules per sample.

Hematoxylin and eosin staining
Mice were euthanized, and testes were collected. The testes were shipped in Excalibur's Alcoholic z-fix (Excalibur Pathology Inc., Norman, OK) for cross-sectioning and hematoxylin and eosin (H&E) staining at Excalibur Pathology. Images of sections stained with H&E were taken with a Nikon Eclipse Ti microscope with DS-Ri2 camera with Plan Apo λ 20x/0.75 NA, Plan fluor 40x/1.30 NA oil, or Plan Apo λ 60X/1.40 NA oil objectives.

RNA extraction and RT-qPCR
For the reverse transcription PCR, P10 testes were collected in 200 µL of TRIzol and frozen in dry ice. According to the manufacturer's recommendations, RNA was extracted using an RNA purification kit (Invitrogen) with on-column DNase treatment (Invitrogen). Subsequently, 1 µg of purified RNA was used for cDNA synthesis using SuperScript IV VILO Master Mix (Invitrogen). For quantitative PCR (qPCR), 5 ng of the synthesized cDNA was combined with 250 nM of forward and 250 nM of reverse primers and SYBR Green qPCR Master Mix (Agilent Technologies). The reference genes used were *Yhwaz*, *Polr2b*, and *Atp5b*. The PCR amplification efficiencies for each primer set were confirmed to be between 90 and 110%. The ΔΔCt method, which included primer efficiencies for the reference and target genes, was used to analyze qPCR data[35,36]. qPCR was performed using either Stratagene MX3000p or Bio-Rad CFX96 cyclers. Primer sequences are listed in (Table S2).

Statistical analysis
Statistical analyses were performed in OriginPro software. All data are represented as mean ± standard error of the mean (SEM). All data are a representation of a minimum of three independent experiments. Immunoblot, qPCR, spermatogonia cell count and testes weight were analyzed by unpaired t-test (two-tailed).

Data availability
All data generated or analysed during this study are included in this published article.

Received: 19 April 2024; Accepted: 27 August 2024
Published online: 07 September 2024

References
1. Goodson, H. V. & Jonasson, E. M. Microtubules and microtubule-associated proteins. *Cold Spring Harb. Perspect. Biol.* https://doi.org/10.1101/cshperspect.a022608 (2018).
2. Barlan, K. & Gelfand, V. I. Microtubule-based transport and the distribution, tethering, and organization of organelles. *Cold Spring Harb. Perspect. Biol.* https://doi.org/10.1101/cshperspect.a025817 (2017).
3. Breuss, M. *et al.* Mutations in the β-tubulin gene TUBB5 cause microcephaly with structural brain abnormalities. *Cell Rep.* **2**, 1554–1562. https://doi.org/10.1016/j.celrep.2012.11.017 (2012).
4. Luscan, R. *et al.* Mutations in TUBB4B cause a distinctive sensorineural disease. *Am. J. Hum. Genet.* **101**, 1006–1012. https://doi.org/10.1016/j.ajhg.2017.10.010 (2017).
5. Feng, R. *et al.* Mutations in TUBB8 and human oocyte meiotic arrest. *N. Engl. J. Med.* **374**, 223–232. https://doi.org/10.1056/NEJMoa1510791 (2016).
6. Bahi-Buisson, N. *et al.* The wide spectrum of tubulinopathies: What are the key features for the diagnosis?. *Brain* **137**, 1676–1700. https://doi.org/10.1093/brain/awu082 (2014).
7. Hurd, D. D., Miller, R. M., Núñez, L. & Portman, D. S. Specific α- and β-tubulin isotypes optimize the functions of sensory cilia in caenorhabditis elegans. *Genetics* **185**, 883–896. https://doi.org/10.1534/genetics.110.116996 (2010).
8. Silva, M. *et al.* Cell-specific α-tubulin isotype regulates ciliary microtubule ultrastructure, intraflagellar transport, and extracellular vesicle biology. *Curr. Biol.* **27**, 968–980. https://doi.org/10.1016/j.cub.2017.02.039 (2017).
9. Griswold, M. D. Spermatogenesis: The commitment to meiosis. *Physiol. Rev.* **96**, 1–17. https://doi.org/10.1152/physrev.00013.2015 (2016).
10. Fayomi, A. P. & Orwig, K. E. Spermatogonial stem cells and spermatogenesis in mice, monkeys and men. *Stem Cell Res.* **29**, 207–214. https://doi.org/10.1016/j.scr.2018.04.009 (2018).
11. O'Donnell, L. & O'Bryan, M. K. Microtubules and spermatogenesis. *Semin. Cell Dev. Biol.* **30**, 45–54. https://doi.org/10.1016/j.semcdb.2014.01.003 (2014).
12. Gadadhar, S., Hirschmugl, T. & Janke, C. The tubulin code in mammalian sperm development and function. *Semin. Cell Dev. Biol.* **137**, 26–37. https://doi.org/10.1016/j.semcdb.2021.12.003 (2023).
13. Lewis, S. A. & Cowan, N. J. Complex regulation and functional versatility of mammalian alpha- and beta-tubulin isotypes during the differentiation of testis and muscle cells. *J. Cell Biol.* **106**, 2023–2033. https://doi.org/10.1083/jcb.106.6.2023 (1988).
14. Buaas, F. W. *et al.* Plzf is required in adult male germ cells for stem cell self-renewal. *Nat. Genet.* **36**, 647–652. https://doi.org/10.1038/ng1366 (2004).
15. Niedenberger, B. A., Busada, J. T. & Geyer, C. B. Marker expression reveals heterogeneity of spermatogonia in the neonatal mouse testis. *Reproduction* **149**, 329–338. https://doi.org/10.1530/rep-14-0653 (2015).
16. Nakata, H., Wakayama, T., Takai, Y. & Iseki, S. Quantitative analysis of the cellular composition in seminiferous tubules in normal and genetically modified infertile mice. *J. Histochem. Cytochem.* **63**, 99–113. https://doi.org/10.1369/0022155414562045 (2015).
17. Zheng, K., Wu, X., Kaestner, K. H. & Wang, P. J. The pluripotency factor LIN28 marks undifferentiated spermatogonia in mouse. *BMC Dev. Biol.* **9**, 38–38. https://doi.org/10.1186/1471-213X-9-38 (2009).
18. Zhou, Q. *et al.* Expression of stimulated by retinoic acid gene 8 (Stra8) in spermatogenic cells induced by retinoic acid: an in vivo study in vitamin A-sufficient postnatal murine testes. *Biol. Reprod.* **79**, 35–42. https://doi.org/10.1095/biolreprod.107.066795 (2008).

19. Dunleavy, J. E. M., O'Bryan, M. K., Stanton, P. G. & O'Donnell, L. The cytoskeleton in spermatogenesis. *Reproduction* **157**, R53–R72. https://doi.org/10.1530/rep-18-0457 (2019).
20. Kemphues, K. J., Kaufman, T. C., Raff, R. A. & Raff, E. C. The testis-specific β-tubulin subunit in drosophila melanogaster has multiple functions in spermatogenesis. *Cell* **31**, 655–670. https://doi.org/10.1016/0092-8674(82)90321-X (1982).
21. Nielsen, M. G., Turner, F. R., Hutchens, J. A. & Raff, E. C. Axoneme-specific beta-tubulin specialization: A conserved C-terminal motif specifies the central pair. *Curr. Biol.* **11**, 529–533. https://doi.org/10.1016/s0960-9822(01)00150-6 (2001).
22. Raff, E. C., Hutchens, J. A., Hoyle, H. D., Nielsen, M. G. & Turner, F. R. Conserved axoneme symmetry altered by a component β-tubulin. *Curr. Biol.* **10**, 1391–1394. https://doi.org/10.1016/S0960-9822(00)00784-3 (2000).
23. Stathatos, G. G. *et al.* Epsilon tubulin is an essential determinant of microtubule-based structures in male germ cells. *EMBO Rep.* **25**, 2722–2742. https://doi.org/10.1038/s44319-024-00159-w (2024).
24. Diggle, C. P. *et al.* A tubulin alpha 8 mouse knockout model indicates a likely role in spermatogenesis but not in brain development. *PLoS ONE* **12**, e0174264. https://doi.org/10.1371/journal.pone.0174264 (2017).
25. Vogel, P., Hansen, G., Fontenot, G. & Read, R. Tubulin tyrosine ligase-like 1 deficiency results in chronic rhinosinusitis and abnormal development of spermatid flagella in mice. *Vet. Pathol.* **47**, 703–712. https://doi.org/10.1177/0300985810363485 (2010).
26. Giordano, T. *et al.* Loss of the deglutamylase CCP5 perturbs multiple steps of spermatogenesis and leads to male infertility. *J. Cell Sci.* https://doi.org/10.1242/jcs.226951 (2019).
27. Ludueña, R. F. A hypothesis on the origin and evolution of tubulin. *Int. Rev. Cell Mol. Biol.* **302**, 41–185. https://doi.org/10.1016/b978-0-12-407699-0.00002-9 (2013).
28. Feng, M. *et al.* Tubulin TUBB4B is involved in spermatogonia proliferation and cell cycle processes. *Genes (Basel)* https://doi.org/10.3390/genes13061082 (2022).
29. Green, C. D. *et al.* A comprehensive roadmap of murine spermatogenesis defined by single-cell RNA-seq. *Dev. Cell* **46**, 651-667. e610. https://doi.org/10.1016/j.devcel.2018.07.025 (2018).
30. Sewell, M. T., Legué, E. & Liem, K. F. Tubb4b is required for multi-ciliogenesis in the mouse. *Development* https://doi.org/10.1242/dev.201819 (2023).
31. Dodd, D. O. *et al.* Ciliopathy patient variants reveal organelle-specific functions for TUBB4B in axonemal microtubules. *Science* **384**, eadf5489. https://doi.org/10.1126/science.adf5489 (2024).
32. Sofroni, K. *et al.* CDKD-dependent activation of CDKA;1 controls microtubule dynamics and cytokinesis during meiosis. *J. Cell Biol.* https://doi.org/10.1083/jcb.201907016 (2020).
33. Mytlis, A., Levy, K. & Elkouby, Y. M. The many faces of the bouquet centrosome MTOC in meiosis and germ cell development. *Curr. Opin. Cell Biol.* **81**, 102158. https://doi.org/10.1016/j.ceb.2023.102158 (2023).
34. Lee, C. Y. *et al.* Mechanism and regulation of rapid telomere prophase movements in mouse meiotic chromosomes. *Cell Rep.* **11**, 551–563. https://doi.org/10.1016/j.celrep.2015.03.045 (2015).
35. Livak, K. J. & Schmittgen, T. D. Analysis of relative gene expression data using real-time quantitative PCR and the 2(-delta delta C(T)) method. *Methods* **25**, 402–408. https://doi.org/10.1006/meth.2001.1262 (2001).
36. Vandesompele, J. *et al.* Accurate normalization of real-time quantitative RT-PCR data by geometric averaging of multiple internal control genes. *Genome Biol.* https://doi.org/10.1186/gb-2002-3-7-research0034 (2002).

Acknowledgements

This work was supported by NIH grants to VR (R01EY031346, R01EY028035), unrestricted challenge grant from Research To Prevent Blindness (RPB) to WVU and the Visual Sciences Center of Biomedical Research Excellence (VS-COBRE Grant P20GM144230). WVU HSC is acknowledged for the predoctoral fellowship awarded to US.

Author contributions

U.S. and V.R. conceptualization; U.S. and V.R. methodology; U.S., N.R.W., and S.B.R. investigation; U.S. and V.R. formal analysis; U.S. and V.R. data curation; U.S.—writing original draft; U.S. and V.R. writing, review, and editing; V.R. supervision; V.R. project administration; V.R. funding acquisition.

Competing interests

The authors declare no competing interests.

Additional information

Supplementary Information The online version contains supplementary material available at https://doi.org/10.1038/s41598-024-71303-8.

Correspondence and requests for materials should be addressed to V.R.